Title

CT ventilation functional image-based IMRT treatment plans are comparable to SPECT ventilation functional image-based plans

Journal

Radiotherapy and Oncology, 118(3)

ISSN

0167-8140

Authors

Kida, Satoshi
Bal, Matthieu
Kabus, Sven
et al.

Publication Date

2016-03-01

DOI

10.1016/j.radonc.2016.02.019

Peer reviewed

Radiotherapy and Oncology 118 (2016) 521–527

Contents lists available at ScienceDirect

Radiotherapy and Oncology

journal homepage: www.thegreenjournal.com

Functional IGRT

CT ventilation functional image-based IMRT treatment plans are comparable to SPECT ventilation functional image-based plans

Satoshi Kida [a,b], Matthieu Bal [c], Sven Kabus [d], Mohammadreza Negahdar [e], Xin Shan [e], Billy W. Loo Jr. [e], Paul J. Keall [f], Tokihiro Yamamoto [a,*]

[a] Department of Radiation Oncology, University of California Davis, Sacramento, USA; [b] Department of Radiation Oncology, Tohoku University School of Medicine, Sendai, Japan; [c] Philips Healthcare, Best, Netherlands; [d] Department of Digital Imaging, Philips Research, Hamburg, Germany; [e] Department of Radiation Oncology, Stanford University, Stanford, USA; [f] Radiation Physics Laboratory, Sydney Medical School, University of Sydney, Australia

ARTICLE INFO

Article history:
Received 15 September 2015
Received in revised form 7 January 2016
Accepted 5 February 2016
Available online 24 February 2016

Keywords:
Lung cancer
Radiation pneumonitis
Lung functional imaging
4D-CT
Deformable image registration

ABSTRACT

Purpose: To investigate the hypothesis that CT ventilation functional image-based IMRT plans designed to avoid irradiating highly-functional lung regions are comparable to single-photon emission CT (SPECT) ventilation functional image-based plans.

Methods and materials: Three IMRT plans were created for eight thoracic cancer patients using: (1) CT ventilation functional images, (2) SPECT ventilation functional images, and (3) anatomic images (no functional images). CT ventilation images were created by deformable image registration of 4D-CT image data sets and quantitative analysis. The resulting plans were analyzed for the relationship between the deviations of CT-functional plan metrics from anatomic plan metrics ($\Delta_{\text{CT-anatomic}}$) and those of SPECT-functional plans ($\Delta_{\text{SPECT-anatomic}}$), and moreover for agreements of various metrics between the CT-functional and SPECT-functional plans.

Results: The relationship between $\Delta_{\text{CT-anatomic}}$ and $\Delta_{\text{SPECT-anatomic}}$ was strong (e.g., $R = 0.94$; linear regression slope 0.71). The average differences and 95% limits of agreement between the CT-functional and SPECT-functional plan metrics (except for monitor units) for various structures were mostly less than 1% and 2%, respectively.

Conclusions: This study demonstrated a reasonable agreement between the CT ventilation functional image-based IMRT plans and SPECT-functional plans, suggesting the potential for CT ventilation imaging to serve as a surrogate for SPECT ventilation in functional image-guided radiotherapy.

 Radiotherapy and Oncology 118 (2016) 521–527

Radiation-induced lung injury has detrimental effects on lung function and is associated with radiation pneumonitis, which is a potentially fatal toxicity and occurs in up to 30% of lung cancer patients treated with radiotherapy [1,2]. Radiotherapy that selectively avoids irradiating highly-functional lung regions may reduce pulmonary toxicity [3–5]. This hypothesis is supported by several reports in the literature. Lung dose–function metrics were found to improve predictive power for pulmonary toxicity compared to dose–volume metrics [6,7]. The mean functional V_{20} (fV_{20}) (percent lung function receiving $\geqslant$20 Gy) for patients who developed Grade $\geqslant$3 pneumonitis was 4.3% greater ($p = 0.09$) than those who did not, and it was closer to statistical significance than the V_{20} (percent lung volume receiving $\geqslant$20 Gy) ($p = 0.33$) [7].

Several modalities exist for pulmonary ventilation imaging [8–11]. Ventilation images can also be acquired by a method based on four-dimensional (4D) computed tomography (CT) and image processing/analysis [12,13], henceforth referred to as CT ventilation imaging. CT ventilation imaging has the potential for widespread clinical implementation, as 4D-CT is routinely acquired for treatment planning at many centers [14] and ventilation computation only involves image processing/analysis without extra scans to patients. Additionally, CT ventilation imaging has a shorter scan time, higher spatial resolution (the exact resolution is unknown), lower cost, and/or greater availability than other modalities.

Validation studies for CT ventilation imaging have been focused on cross-modality image comparisons [15–22]. For example, studies with mechanically ventilated sheep have demonstrated strong correlations between CT ventilation and xenon-CT ventilation [15,16]. Human studies have also reported reasonable correlations with ventilation scintigraphy [21], single-photon emission CT (SPECT) ventilation [22] and other modalities [19,20]. Previously we have demonstrated that CT ventilation in SPECT ventilation-defined defect regions of interest (ROIs) is significantly lower than

* Corresponding author at: Department of Radiation Oncology, University of California Davis School of Medicine, 4501 X St., Sacramento, CA 95817, USA.
E-mail address: toyamamoto@ucdavis.edu (T. Yamamoto).

http://dx.doi.org/10.1016/j.radonc.2016.02.019
0167-8140/

in non-defect ROIs for 16 patients from the same clinical trial used in this study, providing physiological validation of CT ventilation imaging [22]. See Appendix A for a full summary of the previous cross-modality comparison studies. There are limitations in those image comparison studies. First, the analysis was limited to certain ROIs or used ventilation values averaged over certain ROIs in most studies. Functional image-based treatment planning, particularly with the voxel-based optimization scheme used in this study, is influenced by regional function not only in certain ROIs but throughout the lung. Second, it is unclear how image correlations should be interpreted, i.e., what level of correlation is considered sufficiently strong, for applications in treatment planning.

The purpose of this study was to compare CT ventilation functional image-based treatment plans with SPECT ventilation functional image-based plans as an assumed ground-truth based on agreements of dose–volume/function metrics between the two plans, reflecting the overall effect of local differences between the CT ventilation and SPECT ventilation images on optimization. These parameters are directly relevant to radiotherapy, and hence more straightforward to interpret in comparison to image correlations. SPECT ventilation imaging is a widely accepted clinical standard imaging modality for the assessment of regional lung function. We tested the hypothesis that CT ventilation functional image-based intensity-modulated radiotherapy (IMRT) plans are dosimetrically comparable to SPECT ventilation functional image-based plans.

Methods and materials

Patients

The patients for this study were selected from those enrolled in a prospective clinical trial (NCT01034514) approved by an institutional review board. This clinical trial investigated the physiological significance of CT ventilation imaging by comparing with pulmonary function test (PFT) measurements and SPECT ventilation images for patients with thoracic cancer [22]. Out of a total of 18 available patients, we selected eight patients treated with conventionally-fractionated radiotherapy who showed no or non-severe central airway depositions of ^{99m}Tc-labeled diethylenetriamine pentaacetate (DTPA) aerosols in the SPECT ventilation image. The severity of central airway depositions was determined by comparing the mean intensity values in central airways and lung. If the mean intensity in central airways was greater than that in the lung, the patient was classified as severe central airway depositions and was excluded from this study. The average interval between the 4D-CT and SPECT scans was 4 ± 5 days. The average difference in the dose delivered prior to the scan was 1 ± 2 Gy. We consider that effects of such time and dose differences on lung function would be limited. Patient characteristics are shown in Table 1.

CT ventilation imaging

CT ventilation images were created in three steps. The first step was the acquisition of 4D-CT scans using a Discovery ST multislice positron emission tomography (PET)/CT scanner (GE Healthcare, Waukesha, WI) in cine mode, or a Biograph mCT PET/CT scanner (Siemens Healthcare, Malvern, PA) in helical mode. The slice thickness ranged from 2 mm to 3 mm. For reconstruction, the CT images (GE) or projections (Siemens) were sorted into ten respiratory bins by the phase-based method using GE Advantage 4D or Siemens Biograph 40 software. The second step was deformable image registration (DIR) for spatial mapping of the peak-inhale 4D-CT image data set (moving) to the peak-exhale image data set (fixed) using a volumetric elastic DIR method, which was found to have sub-voxel accuracy in the previous studies [23–25]. The same level of accuracy was assumed in this study. Only visual inspection of subtraction images (fixed minus deformed moving) was performed to check for major errors. The final step was to quantify regional volume change for each voxel, yielding a CT ventilation image at the peak-exhale phase. In this study, the following two different metrics were investigated: the Hounsfield unit (HU)-based metric [12,26] and Jacobian-based metric [15], both scaled by a local CT density [20,22]. See Appendix B for further details on the HU-based and Jacobian-based metrics.

SPECT ventilation imaging

^{99m}Tc-DTPA SPECT scans and low-dose CT scans for attenuation correction were acquired in the supine posture on a GE Infinia Hawkeye SPECT/CT scanner. SPECT projections were acquired in a 64 × 64 matrix with an 8.8 × 8.8 mm^2 pixel size and 8.8 mm slice spacing. Further details of SPECT ventilation imaging have been described elsewhere [22].

IMRT optimization for functional image-based treatment planning

A dose–function objective was developed for IMRT optimization in a manner similar to the dose–volume objective [27]. Details are described in Appendix C. Regional ventilation information was incorporated into the dose–function objective as spatially non-uniform weight (importance) factors, w_k (ranging from 0 to 1), which were determined as follows. The CT ventilation images were smoothed using a 3D Gaussian filter kernel (7 × 7 × 3 or 9 × 9 × 3 depending on the CT voxel dimension) to match the expected spatial resolution of the SPECT ventilation images. Then, the smoothed CT ventilation images and original (unsmoothed) SPECT ventilation images were converted into percentile distribution images by replacing the ventilation value of each voxel with the corresponding cumulative distribution function (CDF_k) scaled to the range [0,1] (mean 0.5) in a manner similar to Vinogradskiy et al. [7].

Table 1
Patient characteristics.

Patient	Age (yr)	Gender	Histology	Tumor location	PTV (cm^3)	Lung volume (cm^3)		% SPECT defect volume*
						Peak-exhale	Peak-inhale	
1	65	M	Limited stage SCLC	RUL and mediastinum	780	4097	5435	11
2	80	M	Stage II NSCLC	RUL	406	2353	2996	37
3	51	M	Metastases	Mediastinum	293	2183	3176	17
4	67	F	Stage III NSCLC	Mediastinum	304	1536	1904	21
5	59	M	Stage III NSCLC	LUL and mediastinum	218	2691	3011	30
6	44	M	Stage IV thoracic paraganglioma	Mediastinum	754	2316	2711	10
7	66	M	Stage III NSCLC	LLL and mediastinum	942	2097	2582	27
8	63	F	Metastases	RUL, RLL and mediastinum	161	2234	2617	8

Abbreviations: SCLC = small-cell lung cancer, NSCLC = non-small-cell lung cancer, RUL = right upper lobe. RLL = right lower lobe. LUL = left upper lobe. LLL = left lower lobe.
* Defects were segmented by thresholding with the mean intensity of the background noise plus twice the standard deviation.

When the ventilation value of the voxel, k is denoted by V_k, the weight factor, w_k is given by

$$w_k = CDF_k = \frac{N_k \in [0, V_k]}{N} \quad (1)$$

where N_k is the number of voxels with a ventilation value in the range of [0, V_k]. Finally, those percentile distribution images were resampled at the dose calculation grid spacing ($3 \times 3 \times 3\ mm^3$) for IMRT optimization. The Pinnacle^3 treatment planning system, research version 9.7 (Philips Radiation Oncology Systems, Fitchburg, WI) was used in the current implementation.

CT ventilation functional image-based, SPECT ventilation functional image-based and anatomic image-based treatment planning

Fig. 1 shows a schematic diagram for creating and comparing CT ventilation functional image-based, SPECT ventilation functional image-based, and anatomic image-based IMRT plans. To maintain the scientific rigor and make a fair comparison, only one variable, i.e., the lung weight (importance) factor map, was changed between the three plans and other parameters (number of beams, beam angles and optimization parameters) were kept constant. For all patients, 60 Gy in 30 fractions was prescribed to 95% of the planning target volume (PTV). The clinical target volume (CTV) and PTV were created by adding a gross tumor volume (GTV)-to-CTV margin of 5 mm and a CTV-to-PTV margin of 8 mm, respectively. Nine coplanar, equally-spaced 6-MV photon beams were used. IMRT optimization parameters are shown in Table 2. A spatially non-uniform weight factor map (w_k ranging from 0 to 1, mean 0.5) generated from CT or SPECT ventilation was used for functional image-based planning, while a uniform weight factor map ($w_k = 0.5$ matched with the mean value of a non-uniform weight factor map) was used for anatomic image-based planning.

Table 2
Optimization parameters for CT ventilation functional image-based, SPECT ventilation functional image-based and anatomical image-based IMRT planning.

Structure	Constraint type	Dose (Gy)	Volume (%)	Weight
PTV	Minimum DVH	60	95	100
PTV	Minimum dose	54		40
PTV	Maximum dose	72		40
PTV	Minimum dose	60		10
PTV	Maximum dose	60		10
Heart	Maximum DVH	40	50	20
Heart	Maximum DVH	40	25	1
Spinal cord PRV	Maximum dose	45		50
Esophagus PRV	Maximum DVH	55	30	40
Esophagus PRV	Maximum DVH	40	30	1
Entire thorax minus PTV	Maximum dose	65		100
Total lung minus GTV	Maximum DFH	30	15	0–40 (CT and SPECT)* 20 (anatomical)**
Total lung minus GTV	Maximum DFH	20	25	0–40 (CT and SPECT)* 20 (anatomical)**

Abbreviations: PTV = planning target volume; PRV = planning organ at risk volume; DVH = dose–volume histogram; GTV = gross tumor volume; DFH = dose–function histogram.

* Determined by multiplying the global weight factor of 40 by spatially non-uniform weight factors (ranging from 0 to 1).

** Determined by multiplying the global weight factor of 40 by a spatially uniform weight factor of 0.5.

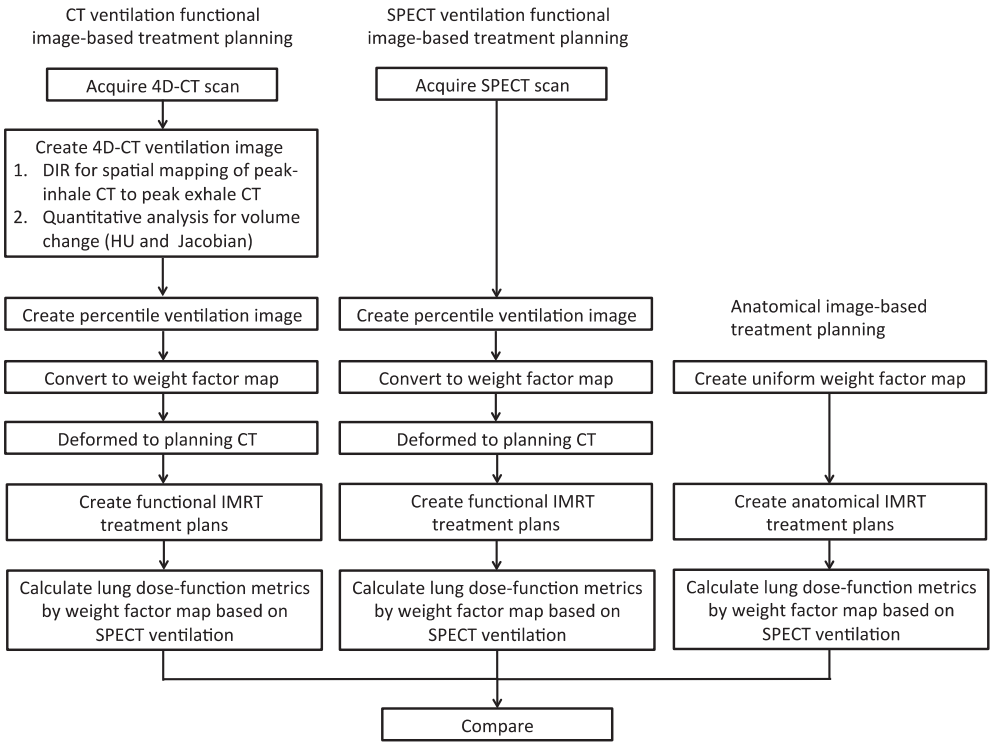

Fig. 1. Schematic diagram for creating and comparing CT ventilation functional image-based, SPECT ventilation functional image-based, and anatomical image-based treatment plans.

The global weight factor was set to 40 for both lung dose–function constraints: fV_{20} < 25% and fV_{30} < 15%. Thus, the weight value of each voxel ranges from 0 to 40 for functional image-based planning, and is 20 for anatomic image-based planning (Table 2). The weight factor maps were deformed to the planning CT image using the displacement vector fields generated by DIR (Demons of Pinnacle[3]) between the peak-exhale 4D-CT image or low-dose CT image of SPECT and the planning CT image. The accuracy of DIR was assessed visually based on the alignment of lung boundaries. Final dose calculation was performed using the adaptive convolution algorithm.

Statistical analysis

To test the hypothesis that CT ventilation functional image-based IMRT plans are comparable to SPECT ventilation functional image-based plans, we quantified the relationship between the deviations of lung dose–function metrics of the CT-functional plan from the anatomic plan ($\Delta_{\text{CT-anatomic}}$) and those of SPECT-functional plan ($\Delta_{\text{SPECT-anatomic}}$) using the Pearson correlation as well as slope from linear regression. We also evaluated the agreements of various dose–volume and dose–function metrics between the CT-functional and SPECT-functional plans using the Bland-Altman method. For the lungs, the following dose–volume metrics were investigated: the mean lung dose (MLD), V_{20}, and effective dose (D_{eff}) [28]. We also calculated the dose–function histogram (DFH) [29] and the following dose–function metrics: fV_{20}, functional MLD (fMLD) [30], and functional effective dose (fD_{eff}) [7]. Vinogradskiy et al. demonstrated a higher predictive power of these dose–function metrics for pneumonitis compared to dose–volume metrics [7]. SPECT ventilation was used to calculate the lung dose–function metrics for all the three plans (Fig. 1). Moreover, we performed secondary analysis to quantify: (1) Spearman's correlations (r_{weight}) between the CT and SPECT ventilation weight factor maps for each patient; (2) Spearman's correlations between the regional weight factor differences (CT – SPECT) and dose differences (CT-functional plan – SPECT-functional plan) for each patient; and (3) the relationship between the r_{weight} and absolute differences in the fV_{20} (CT-functional plan – SPECT-functional plan) for the eight patients.

Results

Fig. 2 shows a comparison of CT ventilation (HU-based) functional image-based and SPECT ventilation functional image-based IMRT plans of two representative patients: Patient 2 showing the smallest difference (0.4%) in the lung fV_{20} between the CT-functional and SPECT-functional plans (Fig. 2a), and Patient 6 showing the largest difference (−2.8%) (Fig. 2b). For Patient 2, there were only minimal differences in the lung DVHs or DFHs between the CT-functional and SPECT-functional plans, e.g., V_{20} 26.7% vs. 27.3%; fV_{20} 27.8% vs. 27.4%. CT and SPECT weight factors around the target volume were both relatively high. The correlation between the CT and SPECT weight factor maps was moderate with an r_{weight} of 0.43 (see also Appendix D). For Patient 6, in contrast, the differences in the lung DVHs or DFHs between the CT-functional and SPECT-functional plans were more obvious, e.g., V_{20} 30.9% vs. 34.9%; fV_{20} 26.9% vs. 29.7%. Overall CT weight factors in ventral lung regions were higher than SPECT weight factors, leading to lower doses in those regions in the CT-functional plan compared to the SPECT-functional plan (Fig. 2b). The correlation between the CT and SPECT weight factor maps was relatively weak with an r_{weight} of 0.31.

Fig. 3a shows the relationships between $\Delta_{\text{SPECT-anatomic}}$ and $\Delta_{\text{CT-anatomic}}$ for the fV_{20}. The HU-based CT ventilation demonstrated a stronger correlation (R = 0.94) and a slope from linear regression (0.71) closer to unity compared to the Jacobian-based CT ventilation (R = 0.85; slope 0.56). $\Delta_{\text{SPECT-anatomic}}$ varied widely with individual subjects, ranging from −11.3% to 2.5%. Positive $\Delta_{\text{SPECT-anatomic}}$ (higher fV_{20} in SPECT-functional plans than in anatomic plans) was observed in two subjects, in which the fV_{20} of the anatomic plans were already lower than or close to the constraints used in optimization. Fig. 3b shows the Bland-Altman plots comparing the fV_{20} of the CT-functional and SPECT-functional plans. The average differences were positive (higher in CT-functional plans than in SPECT-functional plans) and smaller than 1% for both the HU-based and Jacobian-based CT ventilation. The 95% limit of agreement for the HU-based CT ventilation (1.2%) was smaller than that for the Jacobian-based CT ventilation (1.7%). Four patients (1, 5, 6 and 7) showed relatively large differences greater than 2% for the Jacobian-based CT ventilation (absolute difference range 2.6–3.8%). Those differences were much smaller for the HU-based CT ventilation (absolute difference range 1.4–2.8%).

Table 3 shows the average differences and 95% limits of agreement between the CT-functional and SPECT-functional plan metrics for various metrics. Overall the differences between the CT-functional and SPECT-functional plans were small. For most metrics, the average differences were less than 1% for both the HU-based and Jacobian-based CT ventilation. The limits of agreement for the HU-based CT ventilation were smaller than the Jacobian-based CT ventilation consistently for most metrics.

See Appendix D for the results of secondary analysis. Key results are as follows: (1) the mean r_{weight} was 0.40 for the HU-based CT ventilation and 0.37 for the Jacobian-based CT ventilation; (2) overall there were only weak correlations between the regional weight factor differences and dose differences (mean −0.24 for HU; −0.25 for Jacobian); and (3) the correlations between the r_{weight} and fV_{20} absolute differences were found to be moderate (−0.47) for the HU-based CT ventilation, suggesting that the difference between the CT and SPECT-functional plans decreases with increasing correlation between the CT and SPECT ventilation weight factor maps. However, there was almost no correlation (0.14) for the Jacobian-based CT ventilation.

Discussion

This study demonstrated a reasonable agreement between the CT ventilation functional image-based treatment plans and SPECT ventilation functional image-based plans. To our knowledge, this is the first dosimetric validation of CT ventilation functional image-based treatment planning against an assumed ground-truth. The results suggest the potential for CT ventilation imaging to serve as a surrogate for SPECT ventilation in functional image-guided radiotherapy.

There are several limitations in this study. First, a small sample size is considered a weakness. In particular, several patients showed little difference between the functional image-based and anatomic image-based plans (see Fig. 3), indicating that functional images had little effect on optimization. Future studies with a larger sample size, specifically including patients who benefit greatly from functional image-based planning would provide further insights into the significance of CT ventilation functional image-based treatment planning. Second, SPECT ventilation images have limited quality due to low resolution and central airway depositions of aerosols. Upsampling was necessary to match the dose calculation grid spacing, which might have affected the results. For future studies, comparison with high-quality ventilation images (e.g., xenon-CT) may provide more insights into dosimetric differences. Third, the accuracy of image registration between the SPECT and planning CT images is limited by the poor quality of low-dose CT images and possibly large anatomic changes between the SPECT and planning CT scans caused by differences in the acquisition time and positioning. Future developments of DIR methods that are

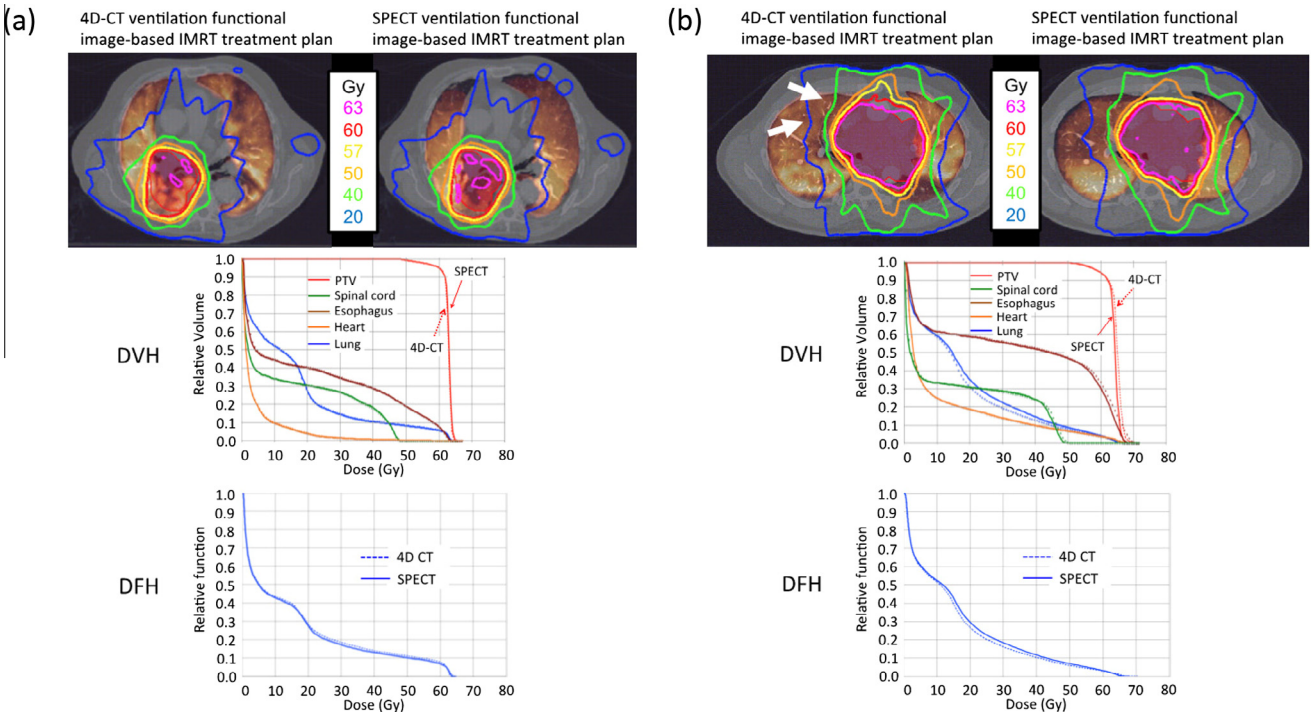

Fig. 2. Example isodose curves, dose–volume histograms (DVHs), and lung dose–function histograms (DFHs) for the CT ventilation (HU-based) functional image-based and SPECT ventilation functional image-based IMRT plans for (a) Patient 2 showing the smallest difference in the lung fV20, and (b) Patient 6 showing the largest difference where the 20-Gy and 30-Gy isodose curves are pushed toward the mediastinum in the CT-functional plan as indicated by white arrows. CT ventilation-defined and SPECT ventilation-defined weight factor maps are overlaid on the planning CT image of the CT-functional and SPECT-functional plans, respectively.

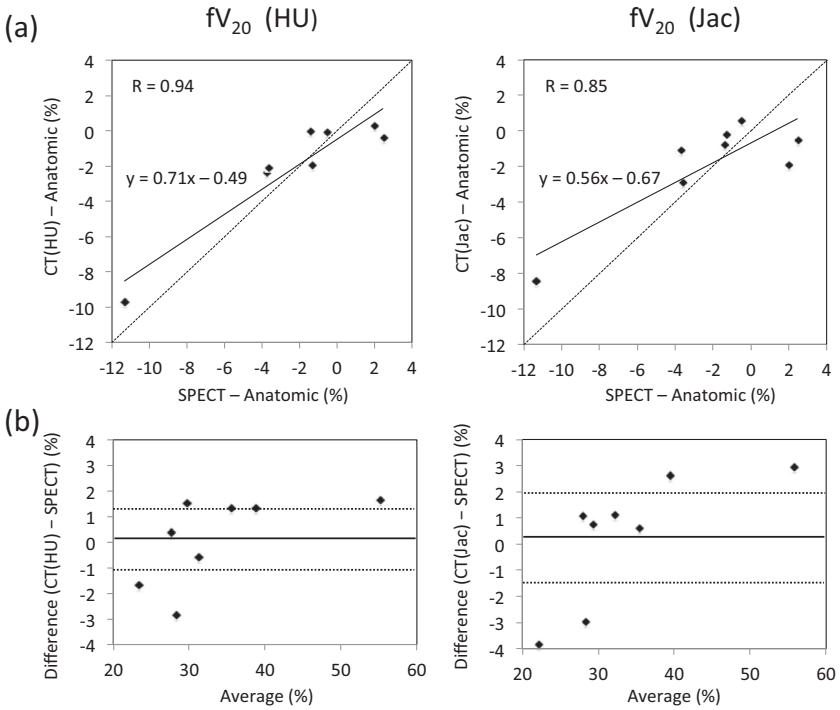

Fig. 3. Comparison of the lung fV_{20} of the CT ventilation (HU-based and Jacobian-based) functional image-based IMRT plans and SPECT ventilation functional image-based plans. (a) Deviations of fV_{20} of the SPECT-functional plan from the anatomical plan ($\Delta_{SPECT\text{-}anatomic}$) vs. those of the CT-functional plan ($\Delta_{CT\text{-}anatomic}$). The lines of unity (dashed lines) and best fit (solid lines) are also shown. (b) Bland-Altman plots comparing the fV_{20} of the CT-functional and SPECT-functional plans. The lines of average difference (solid lines) and 95% limits of agreement (dashed lines) are also shown.

optimized and validated to allow accurate registration for low-dose CT images may reduce uncertainties of the resulting treatment plans. Lastly, CT ventilation imaging itself also has limitations. 4D-CT artifacts have been reported to be an important source of variations in CT ventilation imaging [31]. Also only poor-to-moderate reproducibility has been demonstrated in

Table 3
Dose–volume and dose–function metrics of the CT ventilation (HU-based and Jacobian-based metrics) functional image-based and SPECT ventilation functional image-based IMRT plans for the eight patients.

Metric	CT (HU)	CT (Jac)	SPECT	Average difference ± 95% limit of agreement between CT-functional and SPECT-functional plan (%)	
				HU	Jac
Lung					
MLD (Gy)	19.0 ± 3.3	19.0 ± 3.5	19.2 ± 3.3	−1.1 ± 1.7	−1.2 ± 2.5
V_{20} (%)	35.4 ± 8.5	35.7 ± 9.3	36.3 ± 8.6	−0.8 ± 1.1	−0.6 ± 1.5
Deff (Gy)	25.8 ± 2.4	25.7 ± 2.6	26.0 ± 2.5	−0.9 ± 1.3	−1.1 ± 1.8
fMLD (Gy)	18.3 ± 4.4	18.3 ± 4.6	18.3 ± 4.0	−0.1 ± 2.1	−0.3 ± 3.4
fV_{20} (%)	33.8 ± 10.4	34.0 ± 11.2	33.7 ± 9.4	0.2 ± 1.2	0.3 ± 1.7
fDeff (Gy)	25.0 ± 3.7	25.0 ± 4.0	25.0 ± 3.3	−0.3 ± 1.8	−0.5 ± 2.7
Heart					
V_{40} (%)	13.3 ± 16.0	12.7 ± 14.9	13.6 ± 16.5	−0.3 ± 0.5	−0.9 ± 1.2
Spinal cord					
Maximum dose (Gy)	47.0 ± 4.7	46.8 ± 4.9	47.2 ± 5.1	−0.4 ± 1.6	−0.8 ± 2.0
Esophagus					
Mean dose (Gy)	29.4 ± 8.9	29.3 ± 8.9	29.5 ± 9.2	−0.1 ± 1.1	−0.4 ± 1.2
PTV					
Mean dose (Gy)	64.5 ± 2.2	64.3 ± 2.3	64.4 ± 2.6	0.3 ± 0.7	−0.1 ± 0.7
Homogeneity	1.1 ± 0.1	1.1 ± 0.1	1.1 ± 0.1	0.4 ± 1.0	−0.2 ± 1.0
Monitor units (MUs)	509 ± 118	504 ± 107	509 ± 116	−0.0 ± 3.3	−0.5 ± 3.5

human studies [32,33], which is, at least in part, caused by 4D-CT artifacts or respiratory variations during 4D-CT scans [33]. Future developments of strategies to improve 4D-CT may increase the accuracy and reproducibility of CT ventilation imaging.

Only a single method of functional image-based treatment planning was investigated in this study. There are many other possible methods for ventilation-to-weight transformations, optimization schemes (region-based or voxel-based), objectives and constraints. The ventilation-to-weight transformation method used in this study is similar to Vinogradskiy et al. [7], which did not reach statistical significance for correlations between the lung dose–function metrics and Grade $\geqslant$3 pneumonitis. There are many other possible methods for ventilation-to-weight transformation. They might have observed significant results using a different transformation method. Bowen et al. investigated the sensitivity of IMRT dose painting plans to the mathematical forms of prescription functions (including linear, square root, quadratic and sigmoid transformations) that transform a PET hypoxia image into a map of prescribed doses [34]. Similar studies for CT ventilation functional image-based treatment planning would be an important subject of future work.

The impact of ventilation functional image-guided radiotherapy would vary with regional ventilation, target size, location, and/or delivery technique. Several investigators explored how the dosimetric benefit varies with such factors. For example, Seppenwoolde et al. [35], Christian et al. [36], and Shioyama et al. [37] reported that SPECT perfusion functional image-based treatment planning resulted in a greater degree of sparing of highly-functional regions for patients with large perfusion defects. Munawar et al. reported that SPECT ventilation functional image-based treatment planning resulted in a greater degree of sparing of highly-functional regions when overlap between the highly-functional regions and PTV was minimal and the PTV was not surrounded by highly-functional regions [38]. For future work, the sensitivity of the difference between the CT-functional and SPECT-functional plans should be investigated using a larger sample size with a broad spectrum of regional ventilation patterns, target sizes and locations.

Conclusion

This study provided the first dosimetric validation of CT ventilation functional image-based treatment planning and demonstrated a reasonable agreement with SPECT ventilation functional image-based treatment plans as an assumed ground-truth. The results suggest the potential for CT ventilation imaging to serve as a surrogate for SPECT ventilation imaging in functional image-guided radiotherapy.

Conflict of interest statement

Dr. Bal and Dr. Kabus are employees of Philips. Dr. Keall is an inventor of the issued patent, Method and system for using computed tomography to test pulmonary function (US 7668357).

Acknowledgments

This study was supported in part by the Free to Breathe Young Investigator Research Grant, NIH/NCI R01 CA 093626, and the Japan Society for the Promotion of Science (JSPS) Research Fellowship 127100000646. Philips Radiation Oncology Systems loaned us a research version of the Pinnacle^3 treatment planning system.

Appendix A–D. Supplementary data

Supplementary data associated with this article can be found, in the online version, at http://dx.doi.org/10.1016/j.radonc.2016.02.019.

References

[1] Palma DA, Senan S, Tsujino K, Barriger RB, Rengan R, Moreno M, et al. Predicting radiation pneumonitis after chemoradiation therapy for lung cancer: an international individual patient data meta-analysis. Int J Radiat Oncol Biol Phys 2013;85:444–50.
[2] Marks LB, Bentzen SM, Deasy JO, Kong FM, Bradley JD, Vogelius IS, et al. Radiation dose–volume effects in the lung. Int J Radiat Oncol Biol Phys 2010;76:S70–6.
[3] McGuire SM, Zhou S, Marks LB, Dewhirst M, Yin FF, Das SK. A methodology for using SPECT to reduce intensity-modulated radiation therapy (IMRT) dose to functioning lung. Int J Radiat Oncol Biol Phys 2006;66:1543–52.
[4] Yaremko BP, Guerrero TM, Noyola-Martinez J, Guerra R, Lege DG, Nguyen LT, et al. Reduction of normal lung irradiation in locally advanced non-small-cell lung cancer patients, using ventilation images for functional avoidance. Int J Radiat Oncol Biol Phys 2007;68:562–71.
[5] Yamamoto T, Kabus S, von Berg J, Lorenz C, Keall PJ. Impact of four-dimensional computed tomography pulmonary ventilation imaging-based functional avoidance for lung cancer radiotherapy. Int J Radiat Oncol Biol Phys 2011;79:279–88.

[6] Seppenwoolde Y, De Jaeger K, Boersma LJ, Belderbos JS, Lebesque JV. Regional differences in lung radiosensitivity after radiotherapy for non-small-cell lung cancer. Int J Radiat Oncol Biol Phys 2004;60:748–58.
[7] Vinogradskiy Y, Castillo R, Castillo E, Tucker SL, Liao Z, Guerrero T, et al. Use of 4-dimensional computed tomography-based ventilation imaging to correlate lung dose and function with clinical outcomes. Int J Radiat Oncol Biol Phys 2013;86:366–71.
[8] Simon BA. Regional ventilation and lung mechanics using X-Ray CT. Acad Radiol 2005;12:1414–22.
[9] van Beek EJ, Wild JM, Kauczor HU, Schreiber W, Mugler 3rd JP, de Lange EE. Functional MRI of the lung using hyperpolarized 3-helium gas. J Magn Reson imaging 2004;20:540–54.
[10] Harris RS, Schuster DP. Visualizing lung function with positron emission tomography. J Appl Physiol 2007;102:448–58.
[11] Petersson J, Sanchez-Crespo A, Larsson SA, Mure M. Physiological imaging of the lung: single-photon-emission computed tomography (SPECT). J Appl Physiol 2007;102:468–76.
[12] Guerrero T, Sanders K, Noyola-Martinez J, Castillo E, Zhang Y, Tapia R, et al. Quantification of regional ventilation from treatment planning CT. Int J Radiat Oncol Biol Phys 2005;62:630–4.
[13] Guerrero T, Sanders K, Castillo E, Zhang Y, Bidaut L, Pan T, et al. Dynamic ventilation imaging from four-dimensional computed tomography. Phys Med Biol 2006;51:777–91.
[14] Simpson DR, Lawson JD, Nath SK, Rose BS, Mundt AJ, Mell LK. Utilization of advanced imaging technologies for target delineation in radiation oncology. J Am Coll Radiol 2009;6:876–83.
[15] Reinhardt JM, Ding K, Cao K, Christensen GE, Hoffman EA, Bodas SV. Registration-based estimates of local lung tissue expansion compared to xenon CT measures of specific ventilation. Med Image Anal 2008;12:752–63.
[16] Fuld MK, Easley RB, Saba OI, Chon D, Reinhardt JM, Hoffman EA, et al. CT-measured regional specific volume change reflects regional ventilation in supine sheep. J Appl Physiol 2008;104:1177–84.
[17] Castillo R, Castillo E, Martinez J, Guerrero T. Ventilation from four-dimensional computed tomography: density versus Jacobian methods. Phys Med Biol 2010;55:4661–85.
[18] Castillo R, Castillo E, McCurdy M, Gomez DR, Block AM, Bergsma D, et al. Spatial correspondence of 4D CT ventilation and SPECT pulmonary perfusion defects in patients with malignant airway stenosis. Phys Med Biol 2012;57:1855–71.
[19] Mathew L, Wheatley A, Castillo R, Castillo E, Rodrigues G, Guerrero T, et al. Hyperpolarized (3)He magnetic resonance imaging: comparison with four-dimensional x-ray computed tomography imaging in lung cancer. Acad Radiol 2012;19:1546–53.
[20] Kipritidis J, Siva S, Hofman MS, Callahan J, Hicks RJ, Keall PJ. Validating and improving CT ventilation imaging by correlating with ventilation 4D-PET/CT using (68)Ga-labeled nanoparticles. Med Phys 2014;41:011910.
[21] Vinogradskiy Y, Koo PJ, Castillo R, Castillo E, Guerrero T, Gaspar LE, et al. Comparison of 4-dimensional computed tomography ventilation with nuclear medicine ventilation-perfusion imaging: a clinical validation study. Int J Radiat Oncol Biol Phys 2014;89:199–205.
[22] Yamamoto T, Kabus S, Lorenz C, Mittra E, Hong JC, Chung M, et al. Pulmonary ventilation imaging based on 4-Dimensional computed tomography: comparison with pulmonary function tests and SPECT ventilation images. Int J Radiat Oncol Biol Phys 2014;90:414–22.
[23] Kabus S, Klinder T, Murphy K, van Ginneken B, Lorenz C, Pluim JPW. Evaluation of 4D-CT Lung Registration. In: Yang GZ, Hawkes DJ, Rueckert D, Noble JA, Taylor CJ, editors. Proc of MICCAI. London, UK2009. p. 747–54.
[24] Staring M, Klein S, Reiber JHC, Niessen WJ, Stoel BC. Pulmonary Image Registration with elastix using a Standard Intensity-Based Algorithm. Proc of the Medical Image Analysis For The Clinic - A Grand Challenge, MICCAI2010.
[25] Murphy K, van Ginneken B, Reinhardt JM, Kabus S, Ding K, Deng X, et al. Evaluation of registration methods on thoracic CT: the EMPIRE10 challenge. IEEE Trans Med Imaging 2011;30:1901–20.
[26] Simon BA. Non-invasive imaging of regional lung function using X-ray computed tomography. J Clin Monit Comput 2000;16:433–42.
[27] Wu Q, Mohan R. Algorithms and functionality of an intensity modulated radiotherapy optimization system. Med Phys 2000;27:701–11.
[28] Miften MM, Das SK, Su M, Marks LB. Incorporation of functional imaging data in the evaluation of dose distributions using the generalized concept of equivalent uniform dose. Phys Med Biol 2004;49:1711–21.
[29] Marks LB, Sherouse GW, Munley MT, Bentel GC, Spencer DP. Incorporation of functional status into dose–volume analysis. Med Phys 1999;26:196–9.
[30] Nioutsikou E, Partridge M, Bedford JL, Webb S. Prediction of radiation-induced normal tissue complications in radiotherapy using functional image data. Phys Med Biol 2005;50:1035–46.
[31] Yamamoto T, Kabus S, Lorenz C, Johnston E, Maxim PG, Diehn M, et al. 4D CT lung ventilation images are affected by the 4D CT sorting method. Med Phys 2013;40:101907.
[32] Du K, Bayouth JE, Cao K, Christensen GE, Ding K, Reinhardt JM. Reproducibility of registration-based measures of lung tissue expansion. Med Phys 2012;39:1595–608.
[33] Yamamoto T, Kabus S, von Berg J, Lorenz C, Chung MP, Hong JC, et al. Reproducibility of four-dimensional computed tomography-based lung ventilation imaging. Acad Radiol 2012;19:1554–65.
[34] Bowen SR, Flynn RT, Bentzen SM, Jeraj R. On the sensitivity of IMRT dose optimization to the mathematical form of a biological imaging-based prescription function. Phys Med Biol 2009;54:1483–501.
[35] Seppenwoolde Y, Engelsman M, De Jaeger K, Muller SH, Baas P, McShan DL, et al. Optimizing radiation treatment plans for lung cancer using lung perfusion information. Radiother Oncol 2002;63:165–77.
[36] Christian JA, Partridge M, Nioutsikou E, Cook G, McNair HA, Cronin B, et al. The incorporation of SPECT functional lung imaging into inverse radiotherapy planning for non-small cell lung cancer. Radiother Oncol 2005;77:271–7.
[37] Shioyama Y, Jang SY, Liu HH, Guerrero T, Wang X, Gayed IW, et al. Preserving functional lung using perfusion imaging and intensity-modulated radiation therapy for advanced-stage non-small cell lung cancer. Int J Radiat Oncol Biol Phys 2007;68:1349–58.
[38] Munawar I, Yaremko BP, Craig J, Oliver M, Gaede S, Rodrigues G, et al. Intensity modulated radiotherapy of non-small-cell lung cancer incorporating SPECT ventilation imaging. Med Phys 2010;37:1863–72.